Available online at www.sciencedirect.com
ScienceDirect
Bioorganic & Medicinal Chemistry 16 (2008) 4107–4119
Bioorganic & Medicinal Chemistry

A binary QSAR model for classification of hERG potassium channel blockers

Khac-Minh Thai and Gerhard F. Ecker*

Emerging Field Pharmacoinformatics, Department of Medicinal Chemistry, University of Vienna, Althanstrasse 14, 1090 Vienna, Austria

Received 16 October 2007; revised 6 January 2008; accepted 11 January 2008
Available online 16 January 2008

Abstract—Acquired long QT syndrome causes severe cardiac side effects and represents a major problem in clinical studies of drug candidates. One of the reasons for development of arrhythmias related to long QT is inhibition of the human ether-a-go-go-related-gene (hERG) potassium channel. Therefore, early prediction of hERG K^+ channel affinity of drug candidates is becoming increasingly important in the drug discovery process. Binary QSAR models with threshold values at IC_{50} = 1 and of 10 μM, respectively, were generated using two different sets of descriptors. One set comprising 32 P_VSA descriptors and the other one utilizing a set of descriptors identified out of a large set via a feature selection algorithm. For the full dataset, the power for classification of hERG blockers was 82–88%, which meets prior classification models. Considering the fact that 2D descriptors are fast and easy to calculate, these binary QSAR models are versatile tools for use in virtual screening protocols.

1. Introduction

Almost 35% of all compounds in the drug development pipeline fail due to improper ADMET behavior which renders predictive ADMET an important issue in drug discovery.[1] The tetrameric human ether-a-go-go-related-gene (hERG) protein is a potassium channel which represents an important part of the cardiac action potential.[2–4] Block of the hERG potassium channel may cause acquired long QT syndrome, which leads to Torsades de Points (TdP), a severe cardiac side effect which represents a major problem in clinical studies of drug candidates.[5] Undesirable blockade of the hERG channel was at least in part responsible for the withdrawal of several drugs from the market (e.g., cisapride, terfenadine, astemizole, sertindole, and grepafloxacin).[6–9] Although there are a number of mechanisms other than blocking hERG channels that might be responsible for long QT and especially TdP, hERG activity of compounds under development is a clear no-go signal in the hit to lead process. Therefore, early prediction of hERG K^+ channel affinity of drug candidates is becoming increasingly important in the drug discovery process.[10,11]

Preclinical in vitro and in vivo methods are still imperfect in predicting drug-induced Torsades de Pointes (TdP) in humans. Measuring hERG affinity is via 3*H*-dofetilide binding is routinely performed in HTS-assays, but provides only data focussed on the dofetilide binding site. Other assays, such those utilizing patch–clamp electrophysiology are technically demanding, costly, and labor-intensive.[5] In silico virtual screening procedures to predict hERG binding may develop as a promising tool at least for pre-filtering of large compound libraries.[10,11] Both structure-based and ligand-based approaches have been undertaken to shed more light on the molecular basis of drug–channel interactions. Key amino acid residues being involved in ligand interaction have been identified via a combined protein homology modeling/site directed mutagenesis approach.[12–16] Several X-ray crystal structures of bacterial potassium channels have been solved, including members of the voltage-dependent, calcium-gated, and inward-rectifier families of potassium channels.[17–21] Recently, the MacKinnon group reported the crystal structure of the mammalian Kv channel, Kv1.2, which is a member of the Shaker K^+ channel family (PDB code 2A79).[22] Several publications reported homology models of the human potassium channel which use the bacterium

Keywords: hERG; Potassium channel; Binary QSAR; VSA descriptors; GH score.
* Corresponding author. Tel.: +43 1 4277 55110; fax: +43 1 4277 9551; e-mail: gerhard.f.ecker@univie.ac.at

0968-0896/$ - see front matter © 2008 Elsevier Ltd. All rights reserved.
doi:10.1016/j.bmc.2008.01.017

crystal structures of KcsA (PDB code 1BL8,[17] 1K4C[18]) as template for the closed state and MthK (PDB 1LNQ[19]) as well as KvAP (PDB 1ORQ[20]) for the open state.[12,23–27] Docking studies based on the homology model allowed insights into the drug binding interaction in the inner cavity. Rajamani et al. presented a two-state homology model and demonstrated that flexibility is essential in order to correctly model the binding affinity of a set of diverse ligands.[25] The docking results suggest that blockers bind to the intracellular potassium conduction cavity of hERG via a common mechanism involving extensive hydrophobic and ring stacking interactions with Tyr652 and Phe656.[24]

In the field of ligand-based design, both pharmacophore models and 3D-QSAR models were reported. A preliminary pharmacophore model was described by Ekins et al. using a training set of 15 compounds.[28,29] This hERG pharmacophore model contained four hydrophobic and one positive ionizable feature. A model based on a CoMFA analysis of a set of 31 QT-prolonging drugs comprised a positively charged tertiary amine flanked by three aromatic or hydrophobic centers (Cavalli et al.).[30] These pharmacophore models are quite similar and performed well only on analogues structurally similar to those in the training set. A 3D CoMSiA analysis was performed on a dataset consisting of 22 sertindole analogues and 10 structurally diverse hERG blockers by Pearlstein et al.[31] Based on combined protein homology modeling of the hERG channel pore region and a CoMSiA analysis the authors proposed a 'drain plug' model. However, due to the basic principles of these methods, which require a proper alignment of the ligands, they are neither suited for analysis of structurally diverse compounds nor for virtual screening. Recently, Cianchetta et al. reported 3D-QSAR models using correlation analyses of a large dataset of 882 compounds and pharmacophore-based Grind descriptors.[32] Their 3D-QSAR model for a subset of 338 molecules with non-basic nitrogen atoms had a predictive power (q^2) of 0.72 (322 compounds on training set and 16 molecules for test set). For the ionisable nitrogen subset of 544 molecules (training set/test set = 518:26), the PLS analysis resulted in a model with three latent variables and a $q^2 = 0.74$. These models are quite powerful and showed equal performance than other models based on traditional chemometric methods and Hologram QSAR (HQSAR). Recently, a novel approach by using a panel of plausible pharmacophore hypothesis candidates to constitute the pharmacophore ensemble (PhE) and subject them to regression by support vector machine (SVM) has been reported.[33] The final PhE/SVM model gave an r^2 value of 0.97 for observed versus predicted pIC_{50} values for the training set of 26 compounds, a q^2 value of 0.89 and an r^2 value of 0.94 for the test set of 13 compounds.

In this study, we present binary QSAR models based on the calculation of a set of 32 van der Waals surface area (P_VSA) descriptors and a set of descriptors obtained by a feature selection algorithm for a collection of 313 literature hERG compounds in order to rapidly identify hERG ligands.

2. Results

2.1. Selection of the threshold

For the separation of active/inactive (or blocker/non-blocker), different values of IC_{50} were proposed in the literature as a threshold. Aronov and Goldman chose a cutoff value of 40 μM as a separation point;[34] O'Brien and de Groot and Sun selected values of 20 and 30 μM, respectively.[35,36] Meanwhile several authors proposed substantially lower IC_{50} value for a cutoff (Buyck et al. 130 nM, Song and Clark 316 nM).[37,38] Keserü and Bains et al. opted the active/inactive boundary at $IC_{50} = 1$ μM for their discriminant models.[39,40] Tobita et al. selected both a threshold of 1 and of 40 μM to design two classification models.[41] Fioravanzo et al. separated the dataset for actives and inactives at 10 μM.[42] Last but not least, Roche et al. grouped the dataset into three classes: low IC_{50} class (compounds with $IC_{50} < 1$ μM, blockers), high IC_{50} class (compounds with $IC_{50} \geqslant 10$ μM, non-blockers), and medium IC_{50} class (compounds with $1\ \mu M \leqslant IC_{50} < 10\ \mu M$).[78] The medium IC_{50} value's class ($1\ \mu M \leqslant IC_{50} < 10\ \mu M$) includes some marketed drugs that prolong the QT interval and/or might cause TdP. Several studies showed that compounds with IC_{50} values higher than 10 μM are considered as safe, whereas an IC_{50} value lower than 1 μM is a criteria for discontinuing development.[43] An acceptable degree of safety would be to have a factor of 10- to 30-fold between hERG IC_{50} activity and the plasma concentration used in the clinical setting.[44] However, obviously this cannot be used as dependent variable in QSAR studies as these data are usually not available for large datasets. So it seems reasonable to define the binary threshold at IC_{50} values of 1 or 10 μM, respectively. Therefore, we generated two datasets, one with a pIC_{50} value of 0 as cutoff and one with a pIC_{50} value of −1 as the active/inactive boundary.

2.2. Binary QSAR with threshold = 1 μM

A set of 240 compounds was created as training set to derive a binary QSAR model with a threshold value for active/inactive of 1 μM. Based on this threshold criterion, 81 compounds were classified as active and 159 compounds as inactive. As shown in Table 1 and Table S2, the total accuracies of the two binary QSAR models based on either P_VSA descriptors or 11 2D-descriptors are quite similar with 0.83 for the whole set and 0.80–0.82 for LOO validation. The models show a better performance for inactive compounds than for active ones with GH scores for inactives = 0.88–0.89 and GH score value for actives of 0.72–0.73. For evaluation of the classification power of the binary QSAR models, a test set of 73 compounds was used. Here the model derived from the 11 2D-descriptors performed better than the model based on 32 P_VSA descriptors with total accuracies of 0.93 versus 0.89, respectively. The overall accuracy on the test set was 0.93 with correct predictions for 15 out of 19 active compounds (79%) and 53 out of 54 inactive compounds (98%). Applying the parameters outlined by Jacobsson et al. the precision on active, precision on inactive and enrichment

Table 1. Summary of binary QSAR models

	Threshold IC_{50} = 1 μM				Threshold IC_{50} = 10 μM				High and weak model	
Descriptors/model	VSA[a]	Relevant[b]	VSA[a]	Relevant[b]**I**	VSA[a]	Relevant[b]	VSA[a]	Relevant[b]**II**	VSA[a]	Relevant[b]**III**
Dataset	All		Excl. COOH comp[c]		All		Excl. COOH comp[c]		Excl. COOH comp[c]	
Training set (active/inactive)	240 (81/159)		223 (81/142)		240 (155/85)		223 (155/68)		150 (80/70)	
Total accuracy	0.83	0.83	0.84	0.85	0.80	0.83	0.80	0.83	0.87	0.87
Accuracy on active	0.61	0.65	0.65	0.70	0.90	0.88	0.92	0.90	0.85	0.84
Accuracy on inactive	0.94	0.91	0.94	0.93	0.63	0.73	0.53	0.68	0.90	0.90
Total accuracy LOO[d]	0.82	0.80	0.78	0.81	0.76	0.81	0.78	0.82	0.85	0.84
Accuracy on active LOO[d]	0.58	0.61	0.56	0.62	0.88	0.88	0.91	0.90	0.83	0.79
Accuracy on inactive LOO[d]	0.94	0.91	0.91	0.92	0.54	0.67	0.47	0.63	0.87	0.90
Precision on active	0.85	0.79	0.87	0.85	0.81	0.86	0.82	0.86	0.91	0.91
Precision on inactive	0.83	0.84	0.83	0.85	0.77	0.78	0.73	0.75	0.84	0.83
Enrichment factor	2.51	2.34	2.39	2.34	1.26	1.33	1.17	1.24	1.70	1.70
GH score on active	0.73	0.72	0.76	0.78	0.85	0.87	0.87	0.88	0.87	0.87
GH score on inactive	0.89	0.88	0.89	0.85	0.70	0.75	0.63	0.72	0.87	0.87
Test set (active/inactive)	73 (19/54)		64 (19/45)		73 (42/31)		64 (42/22)		40 (20/20)	
Total accuracy	0.89	0.93	0.91	0.94	0.69	0.71	0.73	0.75	0.88	0.93
Accuracy on active	0.68	0.79	0.68	0.84	0.86	0.79	0.95	0.86	0.95	0.90
Accuracy on inactive	0.96	0.98	1.00	0.98	0.45	0.61	0.32	0.55	0.80	0.95
Precision on active	0.87	0.94	1.00	0.94	0.68	0.73	0.72	0.78	0.83	0.95
Precision on inactive	0.90	0.93	0.88	0.94	0.70	0.68	0.78	0.67	0.94	0.90
Enrichment factor	3.33	3.60	3.37	3.17	1.18	1.27	1.14	1.23	1.65	1.89
GH score on active	0.78	0.86	0.84	0.89	0.77	0.76	0.84	0.82	0.89	0.92
GH score on inactive	0.93	0.96	0.94	0.96	0.58	0.65	0.55	0.61	0.87	0.92
Whole dataset (active/inactive)	313 (100/213)		287 (100/187)		313 (197/116)		287 (197/90)		190 (100/90)	
Total accuracy	0.85	0.85	0.85	0.87	0.77	0.80	0.78	0.82	0.87	0.88
Accuracy on active	0.63	0.68	0.66	0.73	0.87	0.86	0.92	0.89	0.87	0.85
Accuracy on inactive	0.95	0.93	0.96	0.94	0.66	0.70	0.48	0.64	0.88	0.91
Precision on active	0.85	0.82	0.89	0.87	0.75	0.83	0.79	0.85	0.89	0.91
Precision on inactive	0.85	0.86	0.84	0.87	0.81	0.75	0.74	0.73	0.86	0.85
Enrichment factor	2.66	2.56	2.56	2.49	1.38	1.32	1.16	1.23	1.69	1.74
GH score on active	0.74	0.75	0.78	0.80	0.81	0.85	0.86	0.87	0.88	0.88
GH score on inactive	0.90	0.90	0.90	0.90	0.73	0.72	0.61	0.69	0.87	0.88

[a] P_VSA: a set of 32 P_VSA descriptors.
[b] A set of 11 relevant descriptors.
[c] Dataset without –COOH containing compounds.
[d] LOO: leave one out cross-validation. The maximum number of components = 8.

factor (EF) values for the test set are 0.94, 0.93, and 3.60, respectively.

It is noteworthy to mention that the two false positives in the P_VSA descriptor model and the false positive in the 11 2D-descriptors model each contain a carboxylic acid moiety. Carboxylic acids are known to decrease affinity for the hERG channel in many series of diverse structural scaffolds,[45,46] and the binary models/descriptors seem to underestimate this effect. Thus, all 26 compounds in the dataset containing carboxylic acid groups were removed and the models were re-calculated. With the new dataset of 287 compounds we applied two different approaches for selection of training and test set. One just kept the previous training set and removed compounds with carboxylic acids (223 compounds for training), the other repeated the diverse subset selection on the whole dataset (230 compounds for training). Both models showed an improvement in classification power of training set and test set with total accuracy values of 83–85% and 89–94%, respectively. The accuracy on actives for the training set was 63–84% with a precision of 98–100% and for the test set the prediction of actives had an accuracy of 66–73% with a precision of 86–92%. The best binary QSAR model with an 1 μM cutoff is those based on a set of 11 2D-descriptors and the training set of 223 compounds (Model I). This model has a high classification power with total accuracy, accuracy on actives, and accuracy on inactives of 0.85, 0.70, and 0.93, respectively (LOO: 0.81, 0.62, and 0.92). For the test set, the GH score for actives was 0.89 with an accuracy of 84% and a 94% chance of correct prediction (precision), and the GH score for inactives was 0.96 with an accuracy of 98% and a precision of 94%.

2.3. Binary QSAR with threshold = 10 μM

The same training sets described above were also used to build binary QSAR models with a threshold IC_{50} value of 10 μM. Also in this case, the binary QSAR models based on the calculation of 11 2D-descriptors showed better performance than those using P_VSA descriptors. As given in Table 1, the best binary model for classification of hERG blockers at this threshold was obtained

from the training set of 223 compounds utilizing the 11 2D-descriptors (Model II). The cross-validated overall accuracy on the training set is 83% with 90% of actives and 68% of inactives correctly classified (LOO: 82%, 90%, and 63%). On the test set of 64 compounds, the overall accuracy is 75% with correct prediction of 36 out of 42 active compounds (86%) and 12 out of 22 inactive compounds (55%). Comparing the GH scores, the models generally showed a better power in classifying active compounds (GH score = 0.81–0.87) than inactive ones (GH score = 0.61–0.73).

2.4. Binary QSAR with strong and weak hERG blockers (IC_{50} < 1 μM or IC_{50} > 10 μM)

In Model I (threshold = 1 μM), 9 out of 10 false positive in the training set and the false positive in the test set belong to class 3 (IC_{50} in the range of 1–10 μM). The same problem accounts also for Model II (threshold = 10 μM), with 10 out of 15 false negatives in the training set and 5 out of 6 false negative in the test set belonging to the group of moderate hERG affinity compounds. This observation stresses the difficulty to properly classify compounds with moderate hERG activity. Therefore we omitted class 3 and recalculated the models using the same two sets of descriptors. The molecules were split into training (150 compounds) and test (40 compounds) sets by diverse subset selection procedure. Using a set of P_VSA descriptors, the binary model was able to successfully classify the compounds from the training set with an overall accuracy of 87% and to correctly predict 95% and 80% of actives and inactives from the test set, respectively. Similarly, also the binary QSAR model based on the 11 2D-descriptors gave very good results (Model III: total accuracy 0.87, accuracy on actives 0.84, accuracy on inactives 0.90). Moreover, the 2D-descriptor based model showed excellent classification power on the test set (accuracy on actives 0.90 and accuracy on inactives 0.95). It is further noteworthy that the GH scores of Model III for active and inactive compounds keep a high and balanced value with 0.87 for the training set and 0.92 for the test set (Table S2).

2.5. External test set

A dataset containing 58 newly synthesized compounds collected from the literature was used as external test set. However, as can be deduced from a principal component analysis, the chemical space of the external test set is well within those of the training set (Fig. 2D). This might be due to the fact that these compounds belong to lead optimization series from different therapeutic areas such as dipepzidyl peptidase IV inhibitor,[47] CCR8 antagonist,[48] Kv1.5 antagonist,[49] dopamine D_4 agonist,[50] leukocyte function associated antigen-1 antagonist,[51] MCH-R1 antagonist,[52,53] NK1 antagonist,[54] and α7-nicotinic acetylcholine receptor agonist[55] (Table S3). Compounds were optimized towards decrease of hERG activity and are thus well located within the drug like chemical space. In some cases there is only percent hERG inhibition at a single concentration available. Using a logit transformation, estimated hERG IC_{50} was calculated from the following equation: estimated $IC_{50} = [(100 - \%A) * C]/\%A$, where $\%A$ is the percent inhibition measured at the concentration C.[56–58] Using our binary classifiers, all three models performed well with total accuracies of 0.84, 0.78, and 0.86, respectively. To check the applicability domain of the models, also a set of seven compounds located far beyond the space was chosen. These are erythromycin derivatives showing low hERG activity. In this case models failed to correctly classify the compounds.

3. Discussion

Alanine-scanning and site-directed mutagenesis in combination with protein modeling, potential energy mapping, and docking studies revealed three residues at the base of the selectivity filter (Thr623, Ser624, and Val625) and four on the same face of the S6 transmembrane helix (Gly648, Tyr652, Phe656, and Val659) to be involved in drug binding. These information were used to guide the generation of pharmacophore models as well as to select molecular descriptors for QSAR studies on hERG blockers. The typical 3D pharmacophore model for hERG blockader contains a basic nitrogen or a positively charged center flanked by aromatic or hydrophobic groups via flexible linkers. In addition, H-bond acceptors play an important role in hERG binding. Recently also a 3D pharmacophore model for uncharged hERG blockers has been established.[59] Some studies were also successful using pharmacophores as descriptors to derive QSAR models.[33,58] However, the pharmacophore or descriptors suggested may vary depending on the molecules, datasets, and techniques used for model derivation. Furthermore, in a recent study the use of pharmacophore models for polyspecific proteins such as hERG is questioned.[24] In our study, two sets of descriptors were selected in order to generate binary QSAR models for hERG ligands. One is a set of 32 P_VSA descriptors, and the other is a set of 11 2D-descriptors selected by QuaSAR-Contingency analysis. In general, the selected descriptors are in agreement with the prior studies with respect to the need for charged and hydrophobic features. Out of the descriptors selected, there are hydrophobic descriptors ($S\log P$, a_hyd, $S\log$P_VSA7, Q_VSA_HYD, PEOE_VSA_HYD) and global molecular descriptors such as diameter (refers to shape and size of molecules), a_heavy (refers to size of molecules), and opr_nrot (refers to number of rotatable bonds). Moreover, the existence of $S\log$P_VSA7 (hydrophobic and hydrophilic interactions), SMR_VSA5 (polarizability, size) is also noteworthy as those van der Waals volume related descriptors account for a small local differences of globally similar molecular descriptors (e.g., $S\log P$). Diameter and the Kier and Hall chi connectivity indices (chi1v_C, chi0_C) suggest that molecular shape is also an essential descriptor for hERG blockers.

The development of QSAR models depends not only on the statistical method but also on the algorithm used for the selection of training and test sets. There are several methods for division of training and test sets from full

datasets including random division, sorted biological activity data and *K*-means clustering for the factor scores of the original variable matrix along with/without biological activity values. From those methods, Leonard and Roy suggested that *K*-means-cluster based division of training and tests sets can be used as a reliable method.[60] In this study, the MOE Diverse Subset tool was applied to assign a ranking order to entries in a hERG database. A large set of 2D descriptors data together with hERG activity values were used to calculate the pair wise distances between all compounds. A subset of the database comprising entries which are farthest from each other (240 of 313 and 230 of 287 chemical structures) was used as training set and the remaining compounds comprised the test set. By using this algorithm, the training set is a large diverse set, not only by means of the chemical structures (e.g., 2D molecular descriptors) but also of the hERG activities and thus represents in an adequate manner of whole dataset.

One of the main problems of discriminance analysis is how to properly validate and judge the models obtained. A good model will have high predictive power not only of active compounds but also of the inactive ones. Values of total accuracy, accuracy on actives and on inactives, precision for actives and inactives, as well as enrichment factors and GH score were used as measure for classification performance. However, none of the parameters should be used as its own to assign the quality of a model. If the number of inactives is much larger than the number of actives, accuracy on inactives generally will be very high. Vice versa, by predicting only a small number of compounds, precision will be very high. Thus, only a high precision together with a high accuracy will established a powerful classification model and it must be clear that those values depend on the ratio between actives and inactives in the dataset. To retrieve a maximum of information both accuracy on actives (also called recall or sensitivity) and accuracy on inactives (specificity) together with precision on actives and inactives were calculated in all runs. Furthermore, we also describe the first use of the GH score on actives and GH score on inactives to evaluate the quality of classification analyses. In this study, the GH score simply represents the mean of accuracy and precision on actives or inactives. The higher the GH score the stronger is the classification power of the models. A classification model will be considered as perfect when both GH scores are close to 1, the maximum possible value. A summary of GH scores of our best models based on a set of 11 2D-descriptors is shown in Table 2. For Model I (threshold $IC_{50} = 1$ μM), the GH score on inactives (0.90) is larger than those on active compounds (0.8). Thus, this model might be useful when the aim is to remove any compound that blocks the hERG channel at a concentration of $IC_{50} > 1$ μM. Contrary to Model I, the Model II with threshold $IC_{50} = 10$ μM has the GH score on inactives (0.69) smaller than GH score for active compounds (0.87). The model has a higher chance for correct classification of compounds with hERG $IC_{50} < 10$ μM. Therefore, this model is useful when the aim is not to eliminate promising and potentially valuable novels.

To utilize the full panel of chemical diversity in the dataset, we also performed Model I on the full set 287 compounds. In this model, 73% (73/100) of the actives, 94% (176/187) of the inactives, and in total 87% (249/287) were correctly classified. The precision values of the whole dataset on actives and inactives are 87% which means that both an active/inactive hERG ligand has a 87% chance for correct classification. Binary analysis of the full dataset using Model II (threshold 10 μM) gave a total accuracy of 82% (234/287), an accuracy on actives of 89% (176/197), and an accuracy on inactives of 64% (58/90). With a precision on actives of 85% the GH score on actives in this model is higher than those inactives. In Model III, the accuracy and precision on actives/inactives are high and in good relation to each other. Eighty five out of 100 (85%) hERG blocker and 82 out of 90 (91%) negative hERG compounds were correct classified, and also the precision values for actives/inactives are very good with 0.91 and 0.85, respectively. However, this model splits 97 compounds in the class with IC_{50} values in the range of 1–10 μM to be 31 hERG positives and 66 hERG negatives.

Analyzing the misclassified compounds in the whole dataset revealed that only five compounds were misclassified as hERG inactives in all three models (Fig. 1): namely almokalant ($IC_{50} = 0.005$ μM), amsacrine ($IC_{50} = 0.210$ μM), ondansetron ($IC_{50} = 0.81$ μM), olanzapine ($IC_{50} = 0.181$ μM), and BMCL20031829_15 ($IC_{50} = 0.011$ μM). Glibenclamide ($IC_{50} = 74$ μM) was misclassified as hERG active. Four out of five compounds misclassified as hERG inactives contain tertiary

Table 2. The GH scores of binary QSAR models

Descriptors: 11 relevant	Model I threshold $IC_{50} = 1$ μM	Model II threshold $IC_{50} = 10$ μM	Model III high and weak model
Training set (active/inactive)	223 (81/142)	223 (155/68)	150 (80/70)
GH score on active	0.78	0.88	0.87
GH score on in active	0.85	0.72	0.87
Test set (active/inactive)	64 (19/45)	64 (42/22)	40 (20/20)
GH score on active	0.89	0.82	0.92
GH score on inactive	0.96	0.61	0.92
Whole dataset (active/inactive)	287 (100/187)	287 (197/90)	190 (100/90)
GH score on active	0.80	0.87	0.88
GH score on inactive	0.90	0.69	0.88

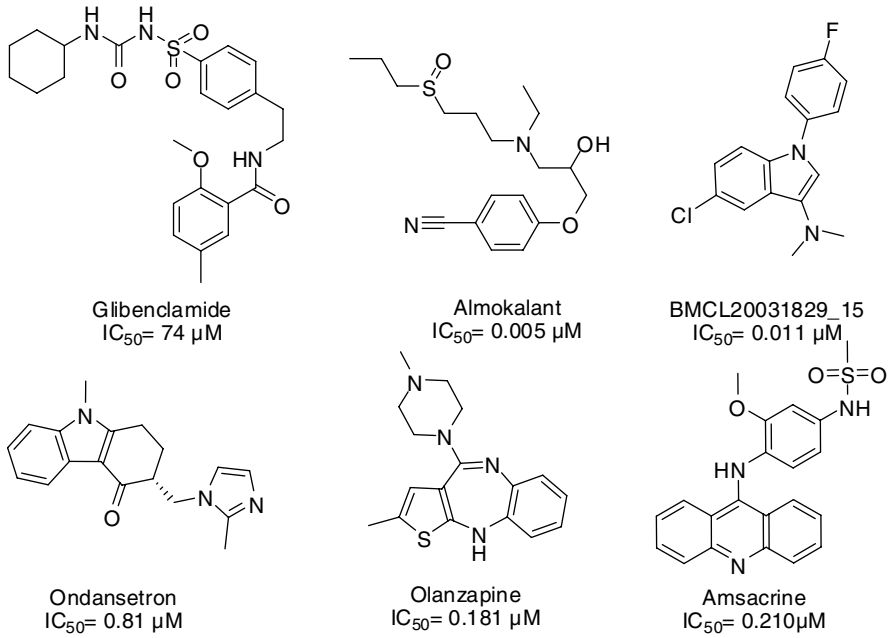

Figure 1. Chemical structures of compounds misclassified in three binary QSAR models.

amino groups, which have been identified as significant contributors for hERG binding in published pharmacophore models[30,28,31] and also a structure-based modeling study.[12] However, these observations should be taken with a grain of salt. *N*-methyl-piperidine shows strong contribution to hERG binding in the Song and Clark study but not in those of Gavaghan et al.[61,38] Furthermore, olanzapine contains a methyl-piperazine ring, which was considered as a chemical fragment typical for in hERG inactive compounds in a fingerprint analysis using LeadScope.[61] Thus, although tertiary amines are associated with high binding, they occur in both strong and weak ($IC_{50} > 10$ μM) hERG binders.

In the dataset, 23 compounds have hERG IC_{50} values obtained from non-mammalian cells (XO). However, only 11 compounds have hERG IC_{50}values larger than 1 μM, hence they may be miscategorized. To develop a model using hERG data obtaining exclusively from mammalian cells, these 11 compounds and also the seven erythromycine analogues that are far beyond the chemical space of the dataset (Fig. 2A) were removed and the remaining compounds were used to generate binary QSAR models. The same protocols described above were applied for this mammalian dataset of 269 compounds. However, to further assess the predictivity and applicability of the models, we additionally split the dataset five times randomly in training and test set (80%/20%), which corresponds to a leave 20% out procedure. Similar results with total accuracies from 0.82–0.92 to 0.70–0.89 for training sets and test sets, respectively (Table S4), were archived for this dataset containing hERG bioactivity from mammalian cells only. To further validation these binary QSAR models, the external testset of 58 compounds (Table S3) and seven erythromycine derivatives which are outside of model boundary were used. Accuracies using the 11 selected descriptors were in the range of 0.81–0.91 for the model with threshold $IC_{50} = 1$ μM, 0.53–0.64 for the model with threshold $IC_{50} = 10$ μM and 0.76–0.79 for the strong and weak hERG blocker model. Lower values of accuracies for the external test set were obtained for models derived from a set of 32 P_VSA descriptors (Table S4). In case of the seven erythromycine derivatives the binary QSAR models failed to correctly classify the compounds as weak hERG binders. Principal component analysis using a set of 11 hERG relevant descriptors shows that these seven natural products are also not in the center of the chemical space of the ChemDiv database (containing 633,864 compounds, 2006)[62] (Fig. 2B). To figure out the differences in terms of chemical structures between hERG actives, middle actives and low actives, SHED profiles[63] of those compounds were calculated using an svl-script available from the Chemical Computing Group svl-exchange program. Dissapointingly, no distinct tendency related to hERG inhibition could be derived (data not shown). This might be due to the fact that very small and minor changes in the chemical features can lead to remarkably altered hERG affinity. When SHED descriptors were applied for the seven hERG inative antibiotic compounds, however, those profiles were different to those from the other compounds, which further strengthens their unique chemical scaffold.

Establishment of 2D-QSAR models seems a reasonable approach for development of predictive screening tools to estimate the hERG binding affinity of drug candidates.[38,39,42,61,64–68] In term of hERG blocker classification, various techniques have been utilized including PLS,[39,42,61] HQSAR,[39] probabilistic neural network (PNN),[69,70] artificial neural network (ANN),[78,35] supervised learning technique and evolutionary computing,[40] support vector machines (SVM),[41,69–71] *k* nearest neighbor (KNN),[70] Bayesian classification,[36] decision tree,[37,70,72,73] and self-organizing maps (SOM).[78,66]

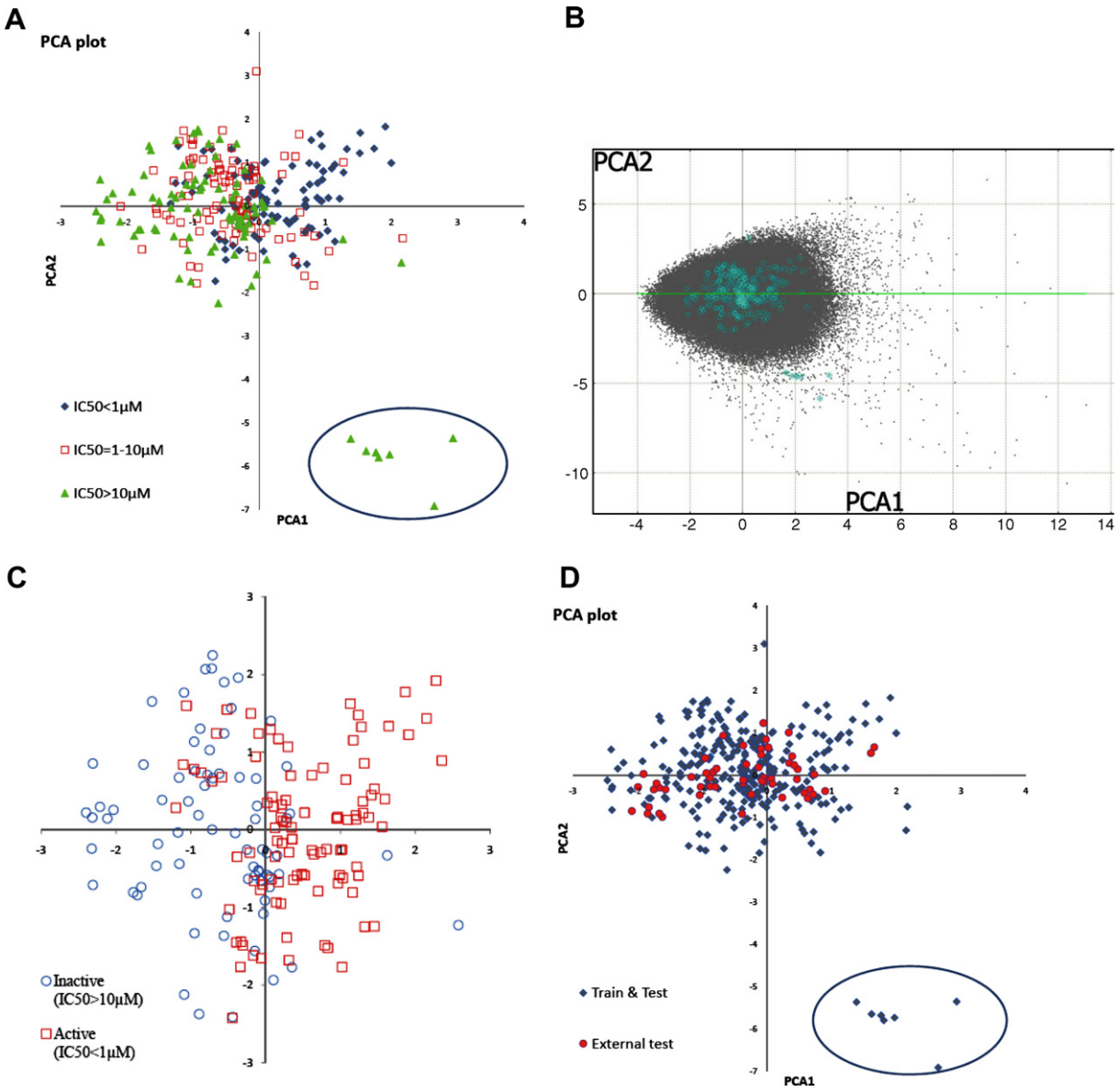

Figure 2. Plot of the first two PCs obtained in a PCA analysis using a set of 11 hERG relevant descriptors. (A) Dataset of 287 compounds with coding according to hERG activity. Compounds outside the model boundary (in ring) were used for validation. (B) Representation of hERG compounds within the chemical space of the ChemDiv database (containing 633,864 compounds, 2006). Grey and cycle dots correspond to the ChemDiv database and hERG compounds, respectively. (C) Dataset of 175 compounds with high and low hERG activity. (D) Chemical space of the training set and external test set used for hERG binary QSAR models.

Table 3 gives an overview on recent results on in silico models for hERG potassium channel blockers and compares them with our binary QSAR models.

Considering the size of the dataset and the structural diversity of the compounds, our results seem acceptable in comparison to other models. It has to be noted, that 10 out of 11 compounds with false positive results in Model I and 15 out of 21 false negatives in Model II had IC_{50} values in the range between 1 and 10 μM. The real life application of our binary classifiers on 58 compounds of an external validation set (Table S3) results in accuracy values of 0.84, 0.78, and 0.86 for Models I, II, III, respectively. Considering the fact, that both P_VSA and also the 11 2D-descriptors are not dependent on the 3D-conformation of the molecules and are fast and easy to calculate (approximately 10^6–10^7 compounds per day on a standard PC), binary QSAR models enable classification of more than 1 million compounds in less than a day on a single Pentium processor machine.

Potent hERG inhibitors often bear a charged amine center that is surrounded by bulky hydrophobic groups. If the charged center is less sterically shielded, for example, through incorporation of alkoxy/hydroxyl groups at the β-position with respect to the amine, it is more easily deprotonated and has lower affinity for hERG.[74] In our binary QSAR models, the set of 11 2D-descriptors that affected the performance of the classification algorithms and related to hERG affinity contains several hydrophobic descriptors (*S*log *P*, a_hyd, *S*logP_VSA7,

Table 3. Summary of published classification QSAR models for hERG blockers

Study	Method	Threshold (μM)	Training set		Test and validation set	
			Comp	Accuracy %	Comp	Accuracy %
Roche et al.[78]	Supervised neural networks	Active < 1 Inactive > 10	244	93[f]	72	71: block[f] 93: non-block[f]
Keserü[39]	PLS (traditional and hologram QSAR)	1	55	83: active	13	85
				87: inactive	82	81–82
Bains et al.[40]	Fragment-based—experimental descriptors and evolutionary algorithm	1	70–100	87–89	22–24	85–90
Aronov and Goldman[34]	2D topological similarity filter and 3D pharmacophore ensemble	40	414 (85 actives, 329 inactive) total accuracy: 82 %[a]			
Yap et al.[70]	Support vector machine	TdP- and non-TdP-causing agent	271	$TdP^{+}_{(LOO)}$: 72 $TdP^{-}_{(LOO)}$: 86	78	TdP^{+}: 97 TdP^{-}: 85 Overall: 91
Gepp and Hutter[72]	Decision tree		264	92–93	75	76–80
Ivanciuc[77]	Artificial immune recognition system (AIRS)	349 (106 TdP^{+}, 243 TdP^{-})	Overall accuracy: 86[b]			
Dubus et al.[73]	Recursive partitioning based on decision tree algorithms	1	160	96–98	60	74–81
		Active < 1 Inactive > 10	100	96–96[f]	55	93–96[f]
Fioravanzo et al.[42]	Consensus score for five PLS-QSAR models	10	29	90	38	82
	Consensus score for five PLS-QSAR and PASS and QikProp models	10	Over all 88 (59/67)			
Tobita et al.[41]	Support vector machine	40 1	73	95[b] 90[b]	827[c]	67–78
O'Brien and de Groot[35]	E-state, 2D fingerprint and neural network	20	46,967	ROC value	11,996	85
	FCFP_6 and Bayesian					82
	Consensus of two models					89[e]
Sun[36]	Universal molecular descriptor system and Bayesian classifier	30	1979	ROC = 0.87[d]	66	88
	FCFP_6 and Bayesian classifier			ROC = 0.95[d]		
Ekins et al.[66]	Kohonen SOM and Sammon non-linear map	Active < 1 Inactive > 10	93	Maps	35	81–95[f]
Model I	11 relevant descriptors and binary analysis	1	223	85 (LOO: 81)	64	94
Model II		10	223	83 (LOO: 78)	64	75
Model III		Active < 1 Inactive > 10	150	87 (LOO: 84)[f]	40	93[f]

[a] 50-fold cross-validation.
[b] 10-fold cross-validation.
[c] TdP- and non-TdP-causing agent, unavailable IC_{50} values.
[d] ROC: receiver operating characteristic.
[e] Accuracy after remove 13% unclassified compounds.
[f] Result for compounds with $IC_{50} < 1$ μM and $IC_{50} > 10$ μM only.

Q_VSA_HYD, PEOE_VSA_HYD). Those descriptors indicate that the hydrophobic nature of molecules has a large impact on hERG blockade and supports the importance of lipophilicity as a factor contributing to hERG potency, which has been presented in many studies.[3,78,40,46,66,75] Simple rules defining lipophilicity thresholds for hERG liability have been derived and lead to the proposal that molecules with $c\log P > 3$ can be optimized by reducing lipophilicity and that compounds having $c\log P$ values < 3 and still exhibit hERG

potency need structural modification.[46,75] However, reduced hERG activity results in most cases from a combination of various factors, and these factors are quite intercorrelated. For example, attenuation of pK_a-values is often accompanied by a reduction of $\log P$, which influences also bioavailability of the compounds. Hence, optimizing the safety profile of a lead compound is always a multifactorial process. Recently, network analysis in MetaCore on antipsychotic ligands with hERG activity indicates that there is an overlap in binding with other promiscuous targets such as CYPs (CYP3A4, CYP2D6, and CYP1A2) and transporters like P-glycoprotein.[76] Thus, drug safety should be considered on a systems level rather than on individual proteins.

4. Conclusions

In drug discovery and development, in silico approaches have the potential to provide cost-effective screening tools for identification of potentially toxic compounds. Within this study we report binary QSAR as a computational method for rapid in silico screening of real and virtual chemical libraries in order to classify compounds with respect to their activity at the hERG K^+ channel. The models derived use 2D molecular descriptors, which are fast and easy to calculate. Quality of the results obtained illustrate the applicability of binary QSAR for classification of hERG actives and thus for identification of potential toxicity risks. However, it has to be stressed that the model, as most models derived from the classical QSAR approach, is only valid within the chemical space of the training set compounds and failed in classifying a small set of erythromycine derivatives. Furthermore, the descriptors used are rather complex and allow only very limited analysis with respect to favorable and unfavorable structural features of the compounds. However, this disadvantage is compensated by the fact that only 2D-structures are needed as input and the descriptors used allow prediction of millions of compounds within one day. Thus, the models might be best used in lead optimization programs for shaping combinatorial libraries in order to decrease the risk for hERG activity.

5. Experimental

5.1. Dataset

The in vitro hERG inhibition data (IC_{50}) for 313 structurally diverse compounds were collected from the literature. Almost all IC_{50} values were measured in mammalian cells (HEK, CHO, and COS). When mammalian cell data were not available (23 out of 313 compounds), IC_{50} measurements from non-mammalian cell lines were used. However, as these are sometimes not comparable and may lead to misleading results, models were established also for the dataset with mammalian cells only. Results show that there are almost no differences in the quality of the models (Table S4, Supporting information). Generally, the pIC_{50} values ($-\log IC_{50}$, concentration in mol/l) were used in statistical analysis. Detailed information including also therapeutic area, cell line used, as well as the corresponding references of all compounds is given in the Supporting information Table S1.

Based upon the IC_{50} value, the dataset was grouped into three classes according to Roche et al.[78] 100 compounds were classified as 1 with $IC_{50} < 1$ μM (low IC_{50}), 116 compounds were assigned to class 2 with $IC_{50} \geqslant 10$ μM (high IC_{50}) and 97 compounds were arranged to class 3 with IC_{50} values in the range of 1–10 μM (medium IC_{50}). Class 1 included some potent hERG K^+-channel blockers known from the literature, such as cisapride, dofetilide, E-4031, haloperidole, and terfenadine. Class 3 also included some marketed drugs that prolong the QT interval and/or might cause TdP. These include amiodarone, chloroquine, chropromazine, desipramine, dolasetron, fentanyl, granisetron, ketoconazole, loratadine, mefloquine, mebefradil, and quinidine.

5.1.1. Training and test set. A total of 313 compounds were used for binary analysis and classified into actives or inactives based on the IC_{50} values and the respective threshold points. In order to create a training and test set, 184 2D molecular descriptors combined with the pIC_{50} value were used to perform a diverse subset selection for the whole dataset using MOE.[79] The 240 most diverse compounds (80%) were used as training set and the remaining 73 structures comprised the test set.

5.2. Computational methods

5.2.1. Molecular descriptors. A wide range of 184 different 2D descriptors including also 32 van der Waals surface area (P_VSA) descriptors were calculated for all compounds using the MOE descriptor tool. 2D molecular descriptors are defined to be numerical properties that can be calculated from the connection table representation of a molecule and included physicochemical properties (14 descriptors), subdivided surface areas (18 descriptors), atom counts and bond counts (41 descriptors), Kier and Hall connectivity and Kappa shape indices (16 descriptors), adjacency and distance matrix descriptors (33 descriptors), pharmacophore feature descriptors (12 descriptors), partial charge descriptors (50 descriptors).

5.2.2. Van der Waals surface area descriptors. P_VSA descriptors are a set of 2D descriptors describing electrostatic, lipophilic, steric, and pharmacophoric properties in terms of the molecular surface.[80] They are quite simple to calculate (neither 3D calculation nor an alignment step is required for the calculation of the descriptors), and thus enable fast in silico screening of large databases of small molecules. The subdivided surface areas are based on an approximate accessible van der Waals surface area calculation for each atom (v_i) along with an atomic property (p_i). The v_i values are calculated using a connection table approximation. Each descriptor in a series is defined to be the sum of the v_i over all atoms i such that p_i is in a specified range $(a, b]$. The atomic properties used include lipophilicity ($S\log P$_VSA0 to $S\log P$_VSA9), molar refractivity (SMR_VSA0 to

Table 4. Description of a set 11 molecular descriptors use to create the binary QSAR models

Property	Name	Description
Adjacency and distance matrix descriptors	Diameter	Largest value in the distance matrix
Atom counts and bond counts	a_heavy	Number of heavy atoms
	opr_nrot	The number of rotatable bonds
Partial charge descriptors	PEOE_VSA_HYD	Total hydrophobic van der Waals surface area
	Q_VSA_HYD	Total hydrophobic van der Waals surface area
Pharmacophore feature descriptors	a_hyd	Number of hydrophobic atoms
Kier and Hall connectivity indices	chi1v_C	Carbon valence connectivity index (order 1)
	chi0_C	Carbon connectivity index (order 0)
Physical properties	*S*log*P*	log of the octanol/water partition
Subdivided surface areas	*S*logP_VSA7	Sum of VSAi with logPi in (0.25,0.30]
	SMR_VSA5	Sum of VSAi with SMRi is in (0.44,0.485]

SMR_VSA7), and partial charge (PEOE_VSA-6 to PEOE_VSA+6). The atomic contributions and the calculation of the descriptors are implemented in the MOE software package version 2006.02.[79]

5.2.3. Feature selection. In order to select the optimum set for the molecular descriptors, QuaSAR-Contingency was applied to prune a set of 184 2D molecular descriptors. A subset of 11 descriptors having an effect on the performance of classification of hERG blockers was selected using correlation analysis, contingency analysis, and uncertainty coefficients (Table 4). In addition, highly correlated descriptors ($r > 0.95$) were removed to avoid redundancy. The remaining descriptors included adjacency and distance matrix descriptors (diameter), atom counts and bond counts (a_heavy, opr_nrot), partial charge descriptors (PEOE_VSA_HYD, Q_VSA_HYD), pharmacophore feature descriptors (a_hyd), Kier and Hall connectivity indices (chi1v_C, chi0_C), physical properties (*S*log*P*) and subdivided surface areas (*S*logP_VSA7, SMR_VSA5).

5.2.4. Binary QSAR analysis. In Binary QSAR, the biological activity is expressed in a 'binary' format (1, active; 0, inactive) and is correlated with molecular descriptors. Briefly, the method estimates the probability density Pr ($Y = 1 \mid X = x$), where Y is a binary variable ($Y = 1$ for an active and $Y = 0$ for an inactive) and X is an n-vector containing the descriptor values (n) for a molecule in the dataset.[81] A binary model assumes that the experimental result is a binary value (1 or 0) representing pass/fail or active/inactive. We used the MOE software package to estimate the above outlined probability density by applying the Bayes' theorem.

5.3. Evaluation criteria for binary models

Performance of the binary QSAR models was measured using standard parameters for classification models. These have been described by Jacobsson et al.[82] and are as follows: (1) the overall classification accuracy of a prediction model, accuracy = (tp + tn)/(tp + fp + tn + fn), (2) accuracy on actives = tp/(tp + fn), and (3) accuracy on inactives = tn/(tn + fp). Within MOE, the quality of a binary QSAR model is generally measured using these three parameters, which are estimated both for the whole set and by applying a cross-validation protocol based on a leave-one-out (LOO) procedure.[83,84,82] We further calculated (4) precision on actives = tp/(tp + fp), (5) precision on inactives = tn/(tn + fn), and (6) enrichment factor EF = precision/[(tp + fn)/(tp + fp + tn + fn)]. In all equations tp = number of true positives, tn = number of true negatives, fp = number of false positives, and fn = number of false negatives. The enrichment factor (EF) indicates the relative enrichment of active compounds in the set of instances predicted to be active in relation to the fraction of active compounds in the original dataset. The EF value is a commonly used parameter in virtual screening and is regarded as good basis for comparison of different methods and models. To assess the quality of a classification model, these parameters should be considered together and none of the above parameters is an absolute measure of classification performance by itself. It has been also suggested that a classifier can only be seen as really successful if high precision is accompanied by high recall. The expected values of the precision and recall for the active class of a random classifier are given by the ratio of actives in the entire set and the ratio between the number of predicted actives and the total number of compounds, respectively.[82,85,86]

5.3.1. GH score. The GH score was used to assess the 'goodness' of hit lists obtained from chemical database searching and from cluster analyses.[87–89] In binary QSAR models, the GH score on actives takes into account both the precision (the fraction of true positives from those predicted as positives) and the percentage

Table 5. Parameters used for evaluation of classification models

Total accuracy	Correct overall prediction (fraction of observations correctly predicted)
Accuracy on actives (recall or sensitivity)	Predicted actives among active subset (fractions of correctly predicted set of actives)
Accuracy on inactives (specificity)	Predicted inactives among inactive subset (fractions of correctly predicted set of inactives)
Precision on actives	Chance that active prediction is correct
Precision on inactives	Chance that inactive prediction is correct
Enrichment factor	Relative enrichment of active compounds in the set of instances predicted to be active in relation to the fraction of active compounds in the original dataset
GH score	Account both of the precision and accuracy

of actives that are retrieved from the dataset. Without a difference of weights describing the relative importance of recall/specificity and precision, the GH score is simply the mean of accuracy and precision. We calculated the GH both for actives and inactives. The original GH score's equation was adapted as follows: (7) GH score for actives = tp[(tp + fp) + (tp + fn)]/2(tp + fp)(tp + fn), (8) GH score for inactives = tn[(tn + fn) + (tn + fp)]/2(tn + fn)(tn + fp). The closer the values are to one, the better the models are. Evaluation criteria for binary models are summarized in Table 5.

Acknowledgments

This work was supported by the PhD program 'Molecular Drug Targets' of the University of Vienna. Khac-Minh Thai thanks the ASEA-Uninet in co-operation with the Austrian Council for Research and Technology Development and the Austrian Academic Exchange Service (ÖAD) for providing a scholarship.

Supplementary data

Summary of all binary QSAR models and dataset of 313 compounds and external test set of 58 compounds with their experimental hERG IC_{50} value (μM), therapeutic area, cell line used, and the literature (four tables). This material is available free of charge via the Internet at www.sciencedirect.com.

Supplementary data associated with this article can be found, in the online version, at doi:10.1016/j.bmc.2008.01.017.

References and notes

1. Pearlstein, R.; Vaz, R.; Rampe, D. *J. Med. Chem.* **2003**, *46*, 2017–2022.
2. Sanguinetti, M. C.; Tristani-Firouzi, M. *Nature* **2006**, *440*, 463–469.
3. Recanatini, M.; Poluzzi, E.; Masetti, M.; Cavalli, A.; De Ponti, F. *Med. Res. Rev.* **2005**, *25*, 133–166.
4. Witchel, H. J. *Expert. Opin. Ther. Targets* **2007**, *11*, 321–336.
5. Hoffmann, P.; Warner, B. *J. Pharmacol. Toxicol. Methods* **2006**, *53*, 87–105.
6. Clancy, C. E.; Kurokawa, J.; Tateyama, M.; Wehrens, X. H.; Kass, R. S. *Annu. Rev. Pharmacol. Toxicol.* **2003**, *43*, 441–461.
7. Jalaie, M.; Holsworth, D. D. *Mini Rev. Med. Chem.* **2005**, *5*, 1083–1091.
8. Fermini, B.; Fossa, A. A. *Nat. Rev. Drug Disc.* **2003**, *2*, 439–447.
9. Finlayson, K.; Witchel, H. J.; McCulloch, J.; Sharkey, J. *Eur. J. Pharmacol.* **2004**, *500*, 129–142.
10. Sanguinetti, M. C.; Mitcheson, J. S. *Trends Pharmacol. Sci.* **2005**, *26*, 119–124.
11. Aronov, A. M. *Drug Discov. Today* **2005**, *10*, 149–155.
12. Mitcheson, J. S.; Chen, J.; Lin, M.; Culberson, C.; Sanguinetti, M. C. *Proc. Natl. Acad. Sci. U.S.A.* **2000**, *97*, 12329–12333.
13. Perry, M.; de Groot, M. J.; Helliwell, R.; Leishman, D.; Tristani-Firouzi, M.; Sanguinetti, M. C.; Mitcheson, J. *Mol. Pharmacol.* **2004**, *66*, 240–249.
14. Witchel, H. J.; Dempsey, C. E.; Sessions, R. B.; Perry, M.; Milnes, J. T.; Hancox, J. C.; Mitcheson, J. S. *Mol. Pharmacol.* **2004**, *66*, 1201–1212.
15. Perry, M.; Stansfeld, P. J.; Leaney, J.; Wood, C.; de Groot, M. J.; Leishman, D.; Sutcliffe, M. J.; Mitcheson, J. S. *Mol. Pharmacol.* **2006**, *69*, 509–519.
16. Kamiya, K.; Niwa, R.; Mitcheson, J. S.; Sanguinetti, M. C. *Mol. Pharmacol.* **2006**, *69*, 1709–1716.
17. Doyle, D. A.; Morais Cabral, J.; Pfuetzner, R. A.; Kuo, A.; Gulbis, J. M.; Cohen, S. L.; Chait, B. T.; MacKinnon, R. *Science* **1998**, *280*, 69–77.
18. Zhou, Y.; Morais-Cabral, J. H.; Kaufman, A.; MacKinnon, R. *Nature* **2001**, *414*, 43–48.
19. Jiang, Y.; Lee, A.; Chen, J.; Cadene, M.; Chait, B. T.; MacKinnon, R. *Nature* **2002**, *417*, 515–522.
20. Jiang, Y.; Lee, A.; Chen, J.; Ruta, V.; Cadene, M.; Chait, B. T.; MacKinnon, R. *Nature* **2003**, *423*, 33–41.
21. Kuo, A.; Gulbis, J. M.; Antcliff, J. F.; Rahman, T.; Lowe, E. D.; Zimmer, J.; Cuthbertson, J.; Ashcroft, F. M.; Ezaki, T.; Doyle, D. A. *Science* **2003**, *300*, 1922–1926.
22. Long, S. B.; Campbell, E. B.; Mackinnon, R. *Science* **2005**, *309*, 897.
23. Choe, H.; Nah, K. H.; Lee, S. N.; Lee, H. S.; Lee, H. S.; Jo, S. H.; Leem, C. H.; Jang, Y. J. *Biochem. Biophys. Res. Commun.* **2006**, *344*, 72–78.
24. Farid, R.; Day, T.; Friesner, R. A.; Pearlstein, R. A. *Bioorg. Med. Chem.* **2006**, *14*, 3160–3173.
25. Rajamani, R.; Tounge, B. A.; Li, J.; Reynolds, C. H. *Bioorg. Med. Chem. Lett.* **2005**, *15*, 1737–1741.
26. Stansfeld, P. J.; Gedeck, P.; Gosling, M.; Cox, B.; Mitcheson, J. S.; Sutcliffe, M. J. *Proteins* **2007**, *68*, 568–580.
27. Tseng, G. N.; Sonawane, K. D.; Korolkova, Y. V.; Zhang, M.; Liu, J.; Grishin, E. V.; Guy, H. R. *Biophys. J.* **2007**, *92*, 3524–3540.
28. Ekins, S.; Crumb, W. J.; Sarazan, R. D.; Wikel, J. H.; Wrighton, S. A. *J. Pharmacol. Exp. Ther.* **2002**, *301*, 427–434.
29. Ekins, S. *Biochem. Soc. Trans.* **2003**, *31*, 611–614.
30. Cavalli, A.; Poluzzi, E.; De Ponti, F.; Recanatini, M. *J. Med. Chem.* **2002**, *45*, 3844–3853.
31. Pearlstein, R. A.; Vaz, R. J.; Kang, J.; Chen, X. L.; Preobrazhenskaya, M.; Shchekotikhin, A. E.; Korolev, A. M.; Lysenkova, L. N.; Miroshnikova, O. V.; Hendrix, J.; Rampe, D. *Bioorg. Med. Chem. Lett.* **2003**, *13*, 1829–1835.
32. Cianchetta, G.; Li, Y.; Kang, J.; Rampe, D.; Fravolini, A.; Cruciani, G.; Vaz, R. J. *Bioorg. Med. Chem. Lett.* **2005**, *15*, 3637–3642.
33. Leong, M. K. *Chem. Res. Toxicol.* **2007**, *20*, 217–226.
34. Aronov, A. M.; Goldman, B. B. *Bioorg. Med. Chem.* **2004**, *12*, 2307–2315.
35. O'Brien, S. E.; de Groot, M. J. *J. Med. Chem.* **2005**, *48*, 1287–1291.
36. Sun, H. *ChemMedChem* **2006**, *1*, 315–322.
37. Buyck, C.; Tollenaere, J.; Engels, M.; De Clerck, F. In *The 14th European Symposium on QSARs*, 8–13 September 2002; Bournemouth, UK.
38. Song, M.; Clark, M. *J. Chem. Inf. Model.* **2006**, *46*, 392–400.
39. Keserü, G. M. *Bioorg. Med. Chem. Lett.* **2003**, *13*, 2773–2775.
40. Bains, W.; Basman, A.; White, C. *Prog. Biophys. Mol. Biol.* **2004**, *86*, 205–233.
41. Tobita, M.; Nishikawa, T.; Nagashima, R. *Bioorg. Med. Chem. Lett.* **2005**, *15*, 2886–2890.
42. Fioravanzo, E.; Cazzolla, N.; Durando, L.; Ferrari, C.; Mabilia, M.; Ombrato, R.; Parenti, M. D. *Internet Electron. J. Mol. Des.* **2005**, *4*, 625–646.
43. Gavaghan, C. L.; Arnby, C. H.; Boyer, S. In *EuroQSAR 2004 Proceedings QSAR and Molecular Modelling in Rational Design of Bioactive Molecules*; Aki, E., Yalcin,

I., Eds.; CADD & Development Society in Turkey: Ankara, 2004; pp 245–246.
44. Redfern, W. S.; Carlsson, L.; Davis, A. S.; Lynch, W. G.; MacKenzie, I.; Palethorpe, S.; Siegl, P. K.; Strang, I.; Sullivan, A. T.; Wallis, R.; Camm, A. J.; Hammond, T. G. *Cardiovasc. Res.* **2003**, *58*, 32–45.
45. Zhu, B. Y.; Jia, Z. J.; Zhang, P.; Su, T.; Huang, W.; Goldman, E.; Tumas, D.; Kadambi, V.; Eddy, P.; Sinha, U.; Scarborough, R. M.; Song, Y. *Bioorg. Med. Chem. Lett.* **2006**, *16*, 5507–5512.
46. Jamieson, C.; Moir, E. M.; Rankovic, Z.; Wishart, G. *J. Med. Chem.* **2006**, *49*, 5029–5046.
47. Pei, Z.; Li, X.; von Geldern, T. W.; Madar, D. J.; Longenecker, K.; Yong, H.; Lubben, T. H.; Stewart, K. D.; Zinker, B. A.; Backes, B. J.; Judd, A. S.; Mulhern, M.; Ballaron, S. J.; Stashko, M. A.; Mika, A. K.; Beno, D. W.; Reinhart, G. A.; Fryer, R. M.; Preusser, L. C.; Kempf-Grote, A. J.; Sham, H. L.; Trevillyan, J. M. *J. Med. Chem.* **2006**, *49*, 6439–6442.
48. Jenkins, T. J.; Guan, B.; Dai, M.; Li, G.; Lightburn, T. E.; Huang, S.; Freeze, B. S.; Burdi, D. F.; Jacutin-Porte, S.; Bennett, R.; Chen, W.; Minor, C.; Ghosh, S.; Blackburn, C.; Gigstad, K. M.; Jones, M.; Kolbeck, R.; Yin, W.; Smith, S.; Cardillo, D.; Ocain, T. D.; Harriman, G. C. *J. Med. Chem.* **2007**, *50*, 566–584.
49. Trotter, B. W.; Nanda, K. K.; Kett, N. R.; Regan, C. P.; Lynch, J. J.; Stump, G. L.; Kiss, L.; Wang, J.; Spencer, R. H.; Kane, S. A.; White, R. B.; Zhang, R.; Anderson, K. D.; Liverton, N. J.; McIntyre, C. J.; Beshore, D. C.; Hartman, G. D.; Dinsmore, C. J. *J. Med. Chem.* **2006**, *49*, 6954–6957.
50. Patel, M. V.; Kolasa, T.; Mortell, K.; Matulenko, M. A.; Hakeem, A. A.; Rohde, J. J.; Nelson, S. L.; Cowart, M. D.; Nakane, M.; Miller, L. N.; Uchic, M. E.; Terranova, M. A.; El-Kouhen, O. F.; Donnelly-Roberts, D. L.; Namovic, M. T.; Hollingsworth, P. R.; Chang, R.; Martino, B. R.; Wetter, J. M.; Marsh, K. C.; Martin, R.; Darbyshire, J. F.; Gintant, G.; Hsieh, G. C.; Moreland, R. B.; Sullivan, J. P.; Brioni, J. D.; Stewart, A. O. *J. Med. Chem.* **2006**, *49*, 7450–7465.
51. Potin, D.; Launay, M.; Monatlik, F.; Malabre, P.; Fabreguettes, M.; Fouquet, A.; Maillet, M.; Nicolai, E.; Dorgeret, L.; Chevallier, F.; Besse, D.; Dufort, M.; Caussade, F.; Ahmad, S. Z.; Stetsko, D. K.; Skala, S.; Davis, P. M.; Balimane, P.; Patel, K.; Yang, Z.; Marathe, P.; Postelneck, J.; Townsend, R. M.; Goldfarb, V.; Sheriff, S.; Einspahr, H.; Kish, K.; Malley, M. F.; DiMarco, J. D.; Gougoutas, J. Z.; Kadiyala, P.; Cheney, D. L.; Tejwani, R. W.; Murphy, D. K.; McIntyre, K. W.; Yang, X.; Chao, S.; Leith, L.; Xiao, Z.; Mathur, A.; Chen, B. C.; Wu, D. R.; Traeger, S. C.; McKinnon, M.; Barrish, J. C.; Robl, J. A.; Iwanowicz, E. J.; Suchard, S. J.; Dhar, T. G. *J. Med. Chem.* **2006**, *49*, 6946–6949.
52. Mendez-Andino, J. L.; Colson, A.-O.; Meyers, K. M.; Mitchell, M. C.; Hodge, K.; Howard, J. M.; Kim, N.; Ackley, D. C.; Holbert, J. K.; Mittelstadt, S. W.; Dowty, M. E.; Obringer, C. M.; Suchanek, P.; Reizes, O.; Eric Hu, X.; Wos, J. A. *Bioorg. Med. Chem.* **2007**, *15*, 2092–2105.
53. Iyengar, R. R.; Lynch, J. K.; Mulhern, M. M.; Judd, A. S.; Freeman, J. C.; Gao, J.; Souers, A. J.; Zhao, G.; Wodka, D.; Doug Falls, H.; Brodjian, S.; Dayton, B. D.; Reilly, R. M.; Swanson, S.; Su, Z.; Martin, R. L.; Leitza, S. T.; Houseman, K. A.; Diaz, G.; Collins, C. A.; Sham, H. L.; Kym, P. R. *Bioorg. Med. Chem. Lett.* **2007**, *17*, 874–878.
54. Thomson, C. G.; Carlson, E.; Chicchi, G. G.; Kulagowski, J. J.; Kurtz, M. M.; Swain, C. J.; Tsao, K.-L. C.; Wheeldon, A. *Bioorg. Med. Chem. Lett.* **2006**, *16*, 811–814.
55. Walker, D. P.; Wishka, D. G.; Piotrowski, D. W.; Jia, S.; Reitz, S. C.; Yates, K. M.; Myers, J. K.; Vetman, T. N.; Margolis, B. J.; Jacobsen, E. J.; Acker, B. A.; Groppi, V. E.; Wolfe, M. L.; Thornburgh, B. A.; Tinholt, P. M.; Cortes-Burgos, L. A.; Walters, R. R.; Hester, M. R.; Seest, E. P.; Dolak, L. A.; Han, F.; Olson, B. A.; Fitzgerald, L.; Staton, B. A.; Raub, T. J.; Hajos, M.; Hoffmann, W. E.; Li, K. S.; Higdon, N. R.; Wall, T. M.; Hurst, R. S.; Wong, E. H.; Rogers, B. N. *Bioorg. Med. Chem.* **2006**, *14*, 8219–8248.
56. Gao, F.; Johnson, D. L.; Ekins, S.; Janiszewski, J.; Kelly, K. G.; Meyer, R. D.; West, M. *J. Biomol. Screen.* **2002**, *7*, 373–382.
57. Yoo, S. E.; Cha, O. J. *Bull. Korean Chem. Soc* **1995**, *16*, 110–112.
58. Johnson, S. R.; Yue, H.; Conder, M. L.; Shi, H.; Doweyko, A. M.; Lloyd, J.; Levesque, P. *Bioorg. Med. Chem.* **2007**, *15*, 6182–6192.
59. Aronov, A. M. *J. Med. Chem.* **2006**, *49*, 6917–6921.
60. Leonard, J. T.; Roy, K. *QSAR Combinat. Sci.* **2006**, *25*, 235–251.
61. Gavaghan, C. L.; Arnby, C. H.; Blomberg, N.; Strandlund, G.; Boyer, S. *J. Comput. Aided Mol. Des.* **2007**, *21*, 189–206.
62. New Chemistry and Discovery Chemistry collections. *ChemDiv*.http://www.chemdiv.com.
63. Gregori-Puigjane, E.; Mestres, J. *J. Chem. Inf. Model* **2006**, *46*, 1615–1622.
64. Aptula, A. O.; Cronin, M. T. *SAR QSAR Environ. Res.* **2004**, *15*, 399–411.
65. Coi, A.; Massarelli, I.; Murgia, L.; Saraceno, M.; Calderone, V.; Bianucci, A. M. *Bioorg. Med. Chem.* **2006**, *14*, 3153–3159.
66. Ekins, S.; Balakin, K. V.; Savchuk, N.; Ivanenkov, Y. *J. Med. Chem.* **2006**, *49*, 5059–5071.
67. Seierstad, M.; Agrafiotis, D. K. *Chem. Biol. Drug Des.* **2006**, *67*, 284–296.
68. Yoshida, K.; Niwa, T. *J. Chem. Inf. Model.* **2006**, *46*, 1371–1378.
69. Chen, X.; Li, H.; Yap, C. W.; Ung, C. Y.; Jiang, L.; Cao, Z. W.; Li, Y. X.; Chen, Y. Z. *Cardiovasc. Hematol. Agents Med. Chem.* **2007**, *5*, 11–19.
70. Yap, C. W.; Cai, C. Z.; Xue, Y.; Chen, Y. Z. *Toxicol. Sci.* **2004**, *79*, 170–177.
71. Bhavani, S.; Nagargadde, A.; Thawani, A.; Sridhar, V.; Chandra, N. *J. Chem. Inf. Model.* **2006**, *46*, 2478–2486.
72. Gepp, M. M.; Hutter, M. C. *Bioorg. Med. Chem.* **2006**, *14*, 5325–5332.
73. Dubus, E.; Ijjaali, I.; Petitet, F.; Michel, A. *ChemMedChem* **2006**, *1*, 662.
74. Zolotoy, A. B.; Plouvier, B. P.; Beatch, G. B.; Hayes, E. S.; Wall, R. A.; Walker, M. J. *Curr. Med. Chem. Cardiovasc. Hematol. Agents* **2003**, *1*, 225–241.
75. Waring, M. J.; Johnstone, C. *Bioorg. Med. Chem. Lett.* **2007**, *17*, 1759–1764.
76. Crumb, W. J., Jr.; Ekins, S.; Sarazan, R. D.; Wikel, J. H.; Wrighton, S. A.; Carlson, C.; Beasley, C. M., Jr. *Pharm. Res.* **2006**, *23*, 1133–1143.
77. Ivanciuc, O. *Internet Electron. J. Mol. Des.* **2006**, *5*, 488.
78. Roche, O.; Trube, G.; Zuegge, J.; Pflimlin, P.; Alanine, A.; Schneider, G. *ChemBioChem* **2002**, *3*, 455–459.
79. MOE 2006.02, Chemical Computing Group Inc., Montreal, H3A 2R7 Canada, http://www.chemcomp.com.
80. Labute, P. *J. Mol. Graph. Model.* **2000**, *18*, 464–467.
81. Labute, P. *Proc. Pacific Symp. Biocomput.* **1999**, 444–455.
82. Jacobsson, M.; Liden, P.; Stjernschantz, E.; Bostrom, H.; Norinder, U. *J. Med. Chem.* **2003**, *46*, 5781–5789.
83. Gao, H.; Williams, C.; Labute, P.; Bajorath, J. *J. Chem. Inf. Comput. Sci.* **1999**, *39*, 164–168.

84. Gao, H.; Lajiness, M. S.; Van Drie, J. *J. Mol. Graph. Model.* **2002**, *20*, 259–268.
85. Baurin, N.; Mozziconacci, J. C.; Arnoult, E.; Chavatte, P.; Marot, C.; Morin-Allory, L. *J. Chem. Inf. Comput. Sci.* **2004**, *44*, 276–285.
86. Prathipati, P.; Saxena, A. K. *J. Chem. Inf. Model.* **2006**, *46*, 39–51.
87. Guner, O. F.; Henry, D. R. In *Pharmacophore Perception Development and Use in Drug Design*; Guner, O. F., Ed.; International University Line: CA, 2000; pp 193–212.
88. Guner, O. F.; Henry, D. R.; Pearlman, R. S. *J. Chem. Inf. Model.* **1992**, *32*, 101–109.
89. Kurogi, Y.; Guner, O. F. *Curr. Med. Chem.* **2001**, *8*, 1035–1055.